

Ultraviolet Absorption Spectra of Ce^{3+} in Alkaline-Earth Fluorides

EUGENE LOH

Physical Sciences Department, Douglas Aircraft Company, Santa Monica, California

(Received 6 September 1966)

The ultraviolet absorption spectra of Ce^{3+} , 0.005%, in crystals of the alkaline-earth fluorides CaF_2 , SrF_2 , and BaF_2 have been measured at both room and liquid-nitrogen temperatures. The general features in the spectra of all three hosts are similar. The ultraviolet spectra of Ce^{3+} , 0.005% to 5%, in CaF_2 show three regions of interconfigurational absorption which may be assigned as: (1) $4f \rightarrow 5d$ bands from about 31 000 to 56 000 cm^{-1} , with half-width about 2000 cm^{-1} at Ce^{3+} concentration $\sim 10^{-2}\%$; (2) $4f \rightarrow 6s$ weak and broad band from 60 000 to about 77 000 cm^{-1} with maximal absorption at about 70 000 cm^{-1} ; and (3) a charge-transfer absorption, $F^-(2p^6) \rightarrow Ce^{3+}(6s)$, appearing as an apparent red shift of the absorption edge of the host CaF_2 at approximately 80 000 cm^{-1} . The assignments of these three regions of absorption are based on the location, width, number, oscillator strength, and temperature dependence of the bands. The effect of large Ce^{3+} concentration, $\geq 0.1\%$, on the uv absorption spectra of Ce^{3+} is interpreted as the result of cluster formation from pairs of Ce^{3+} -interstitial F^- . The vibronic structure in the lowest $4f \rightarrow 5d$ band may be conceived in terms of pseudolocalized vibrations, as in the case of several divalent rare-earth ions in alkali halides treated by Wagner and Bron.

I. INTRODUCTION

AS a direct approach to the study of interconfigurational transitions of trivalent rare-earth (RE) ions, in solids, we have measured the ultraviolet absorption spectra of various RE^{3+} in CaF_2 crystals. Their spectra are similar.¹ The spectrum of Ce^{3+} , however, exhibits more types of interconfigurational transitions than other RE^{3+} in CaF_2 . This is because $Ce^{3+}(4f^1)$, being the lightest ion in the RE^{3+} series, starts its interconfigurational transition $4f \rightarrow 5d$ at the lowest energy.¹ The ultraviolet absorption spectrum of Ce^{3+} in alkaline-earth fluorides will be interpreted in terms of three types of transitions, $4f \rightarrow 5d$, $4f \rightarrow 6s$, and charge transfer of $F^-(2p^6) \rightarrow Ce^{3+}(6s)$. The $4f \rightarrow 5d$ bands occur in the region 31 000 cm^{-1} to 56 000 cm^{-1} , with half-width about 2000 cm^{-1} at Ce^{3+} concentration $\sim 10^{-2}\%$. The weak and broad absorption band between 60 000 cm^{-1} and 77 000 cm^{-1} will be interpreted as $4f \rightarrow 6s$ transition of Ce^{3+} in CaF_2 . The apparent red shift of the absorption edge of $CaF_2:Ce^{3+}$ from that of the undoped CaF_2 , 80 000 cm^{-1} , will be attributed to the charge transfer of $F^-(2p^6) \rightarrow Ce^{3+}(6s)$.

The crystalline environment is expected to have greater effect on interconfigurational transitions of RE^{3+} than on intraconfigurational transitions within the shielded $4f$. This is because the excited states such as $5d$ and $6s$ are not shielded from the surrounding ions. By varying the Ce^{3+} concentration in CaF_2 , the temperature of the crystal, and the host lattice within the alkaline-earth fluorides series we shall demonstrate and interpret these effects on the absorption spectra. We shall discuss the assignments $4f \rightarrow 5d$, $4f \rightarrow 6s$, and charge transfer $F^-(2p^6) \rightarrow Ce^{3+}(6s)$, in the order of increasing photon energy. The effect of crystalline environment on Ce^{3+} absorption constitutes Sec. III on $4f \rightarrow 5d$ absorption of cluster-ion Ce^{3+} in alkaline-earth fluorides.

II. $4f \rightarrow 5d$ ABSORPTION OF SINGLE-ION Ce^{3+} IN ALKALINE-EARTH FLUORIDES

The ultraviolet absorption spectra of 0.005% Ce^{3+} in the alkaline-earth fluorides BaF_2 , SrF_2 , and CaF_2 are shown in Fig. 1 for room and liquid-nitrogen temperatures. The three spectra are similar. However, $BaF_2:Ce^{3+}$ appears to be the simplest. Its spectrum consists of only two regions of absorption, a single-band *A* below 36 000 cm^{-1} and three bands between 47 000 cm^{-1} and 56 000 cm^{-1} , called region *B*. The spectra of $SrF_2:Ce^{3+}$ and $CaF_2:Ce^{3+}$ are very similar to each other. They have additional absorption bands in the intermediate spectral region, a composite band *C* with peak between 41 000 cm^{-1} and 42 000 cm^{-1} and a single band *D* centering between 46 000 cm^{-1} to 47 000 cm^{-1} . It will be shown later that as the concentration of Ce^{3+} in CaF_2 increases the absorption in the intermediate region, *C* and *D*, increases while that in the low-energy *A* and high-energy region *B* decreases. We therefore propose that the latter characterizes the $4f \rightarrow 5d$ absorption¹ of single-ion Ce^{3+} in alkaline-earth fluorides while the former is attributed to the $4f \rightarrow 5d$ absorption of cluster-ion Ce^{3+} in these crystals.

We first discuss the $4f \rightarrow 5d$ absorption of single-ion Ce^{3+} in alkaline-earth fluorides. The absorption of cluster-ion Ce^{3+} will be discussed later in connection with the concentration dependence of Ce^{3+} absorption in CaF_2 . The eightfold coordination of substitutional F^- around Ce^{3+} in alkaline-earth fluorides suggests that the lowest-band *A* be assigned as the $4f \rightarrow 5d(e_g)$ transition and that most of the high bands in *B* correspond to $4f \rightarrow 5d(t_{2g})$. Assuming a tetragonal^{2,3} environment around Ce^{3+} due to the nearest-neighbor interstitial F^- as charge compensator, both e_g and t_{2g} will split into two levels: e_g to (x^2-y^2) and $(2z^2-x^2-y^2)$, and t_{2g} to (xy) and $(yz$ and $zx)$. We therefore assign band

² For example M. J. Weber and R. W. Bierig, Phys. Rev. **134**, A1492 (1964) and references therein.

³ W. Hargreaves (private communication).

¹ E. Loh, Phys. Rev. **147**, 332 (1966); and (unpublished).

TABLE I. $5d$ levels and crystal-field strength $10 Dq$ for single-ion Ce^{3+} in alkaline-earth fluorides.

Host crystal	Experimental data [1000 cm^{-1}] assigned as tetragonal components of $5d$ orbital				Deduced values [1000 cm^{-1}]			Crystal-field strength $10 Dq$
	x^2-y^2	$2z^2-x^2-y^2$	xy	yz and zx	Cubic e_g	t_{2g}	Spherical $5d$	
CaF_2	32.4	49.5	51.1	53.9	41	53	48.2	12
SrF_2	33.6 ⁺	48.8	50.3	53.4	41.2	52.4	48	11.2
BaF_2	34.2	50	51.7 ⁺	53.5	42.1	52.9	48.5	10.8

A as transitions from $4f$ to (x^2-y^2) and the three bands in B as transitions from $4f$ to $(2z^2-x^2-y^2)$, (xy) and $(yz$ and $zx)$ in the order of increasing photon energy.

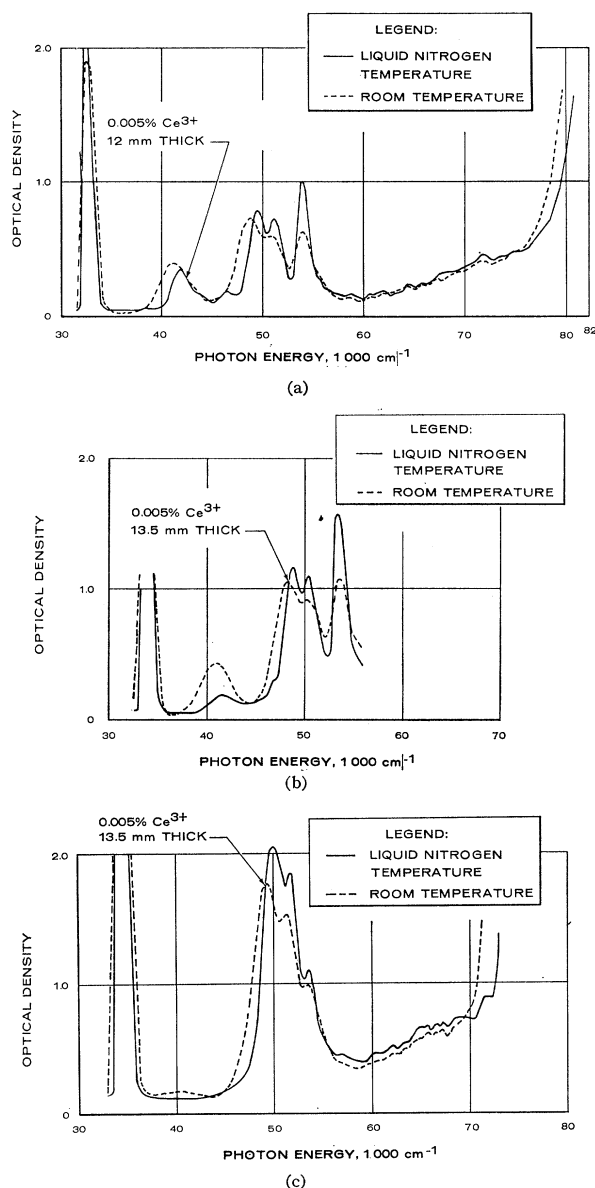


FIG. 1. Ultraviolet absorption spectra of 0.005% Ce^{3+} in (a) CaF_2 , (b) SrF_2 , and (c) BaF_2 at room and liquid-nitrogen temperature.

Table I summarizes the experimental data of $4f \rightarrow 5d$ transitions of single-ion Ce^{3+} in alkaline-earth fluorides at liquid-nitrogen temperature. The data are assigned as components of $5d$ orbital in a tetrahedral environment. The second part of the table lists the centroids of e_g , t_{2g} and $5d$ of Ce^{3+} as deduced from the experimental data,

$$|e_g\rangle = [|x^2-y^2\rangle + |2z^2-x^2-y^2\rangle]/2,$$

$$|t_{2g}\rangle = [|xy\rangle + |yz\rangle + |zx\rangle]/3,$$

and

$$|5d\rangle = [2|e_g\rangle + 3|t_{2g}\rangle]/5.$$

Values of crystal-field strength $10 Dq$ are listed in the last column of the table as the differences in energy between e_g and t_{2g} .

The effects of low temperature on the $4f \rightarrow 5d$ absorption spectra are the sharpening of absorption bands, the increase in separation between the two e_g bands, $|x^2-y^2\rangle$ and $|2z^2-x^2-y^2\rangle$, and the appearance of vibronic structure in the lowest band, $|x^2-y^2\rangle$. Figure 2, with enlarged photon energy scale for clarity, shows the vibronic structure in the $|x^2-y^2\rangle$ band of 0.005% Ce^{3+} embedded in alkaline-earth fluorides at liquid-nitrogen temperature. The locations of the bumps in the structure are summarized in Table II. The data in the table⁴ show that the vibronic structure in each host crystal contains two frequency intervals, a larger interval ω_1 separating "major humps" at ν_j and a smaller spacing

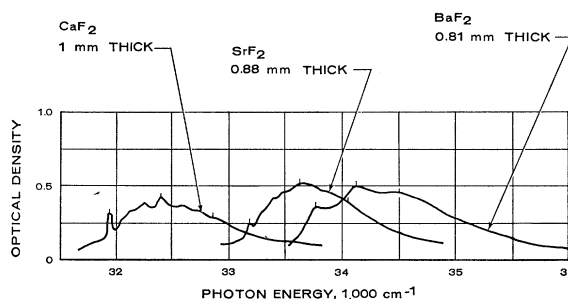


FIG. 2. The lowest $4f \rightarrow 5d$ absorption band of 0.005% Ce^{3+} in CaF_2 , SrF_2 and BaF_2 at liquid-nitrogen temperature.

⁴ Although our data on vibronic structure at liquid-nitrogen temperature are not as detail as that reported by Kaplyanskii *et al.* [Opt. i Spektroskopiya **14**, 664 (1962) [English transl.: Opt. Spectry. (USSR) **14**, 351 (1963)]], with greater spectral resolution and at liquid-helium temperature. However, we shall show that the data appear to be adequate enough to demonstrate several features of the vibronic structure related to the $4f \rightarrow 5d$ transition of trivalent rare earths in alkaline-earth fluorides.

TABLE II. Vibronic structure of 0.005% Ce^{3+} in alkaline earth fluorides at liquid-nitrogen temperature. [Frequency in 1000 cm^{-1} .]

		CaF ₂			
ν_j	31.94			32.4	32.86
ω_1				0.46	0.46
ν_{LO}				0.46	
ν_i	32.1	32.25		32.58	32.73
ω_2	0.16	0.15		0.18	0.15
ν_{ac}	0.07	(Kaiser <i>et al.</i> ^a)			
	0.08	(Kahan <i>et al.</i> ^b)			
		SrF ₂			
ν_j	33.18			33.63	
ω_1				0.45	
ν_{LO}				0.37	
ν_i	33.27	33.37	33.47	33.73	33.84
ω_2	0.09	0.1	0.1	0.1	0.11
ν_{ac}	0.1				
		BaF ₂			
ν_j	33.78			34.14	34.5
ω_1				0.36	0.36
ν_{LO}				0.33	
ν_{ac}	0.09				

^a See Ref. 6.

^b A. Kahan and D. E. McCarthy, Phys. Rev. **142**, 457 (1966).

ω_2 between "minor humps" at ν_i within the interval ω_1 . Both ω_1 and ω_2 decrease as the host crystal changes from CaF₂ toward BaF₂ with increasing lattice parameter.

Wagner and Bron⁵ have observed vibronic structure with larger and smaller frequency separations, ω_1 and ω_2 , in the $4f \rightarrow 5d$ absorption and emission spectra of the divalent rare-earth ions, Sm²⁺, Eu²⁺, and Yb²⁺, in alkali halides at 10°K. They interpreted ω_1 and ω_2 as the resonance frequency of pseudolocalized vibrations occurring at the divalent rare-earth defect in the monovalent host crystal. Their analysis showed that ω_1 is slightly higher than the longitudinal-optical branch, ν_{LO} , and ω_2 is near the peak of the transverse-acoustical branch, ν_{ac} , of the undisturbed host lattice. In order to compare our experimentally deduced values of ω_1 and ω_2 with the values of ν_{LO} and ν_{ac} in the literature, Table II also includes the values of ν_{LO} and ν_{ac} of alkaline-earth fluorides deduced by Kaiser *et al.*⁶ from their infrared measurements. Except for the single discrepancy between $\omega_2 = 160\text{ cm}^{-1}$ and the anomalously low⁷ value of $\nu_{ac} = 70\text{ cm}^{-1}$ for the host CaF₂, there is a general correspondence between ω_1 , ω_2 and ν_{LO} , ν_{ac} for three alkaline-earth fluorides.

The vibronic structure is observed only in the lowest $4f \rightarrow 5d$ band, $|x^2 - y^2\rangle$. This is in agreement with one of two conditions⁸ for observing the pseudolocalized vibronics in doped crystals which have large lattice distortion and strong electron-phonon coupling such as

⁵ M. Wagner and W. E. Bron, Phys. Rev. **139**, A223 (1965).

⁶ W. Kaiser, W. G. Spitzer, R. H. Kaiser, and L. E. Howarth, Phys. Rev. **127**, 1950 (1962).

⁷ The deduced value of ν_{ac} for SrF₂ and BaF₂ are, as shown also in Table II, 99 cm^{-1} and 94 cm^{-1} , respectively. It is not clear why the deduced value of ν_{ac} for CaF₂, 71 cm^{-1} , is lower than that of SrF₂ and BaF₂, instead of higher, as might be expected.

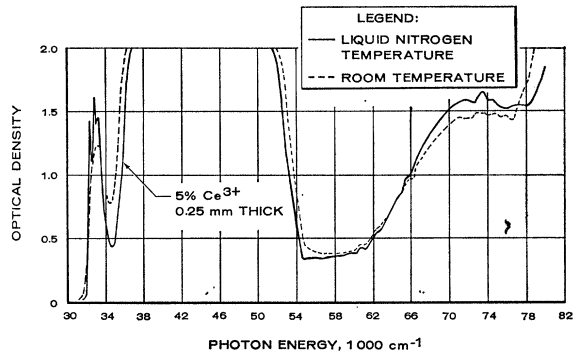
⁸ M. Wagner, Physik Kondensierten Materie **4**, 71 (1965).

rare-earth ion doped alkaline-earth fluorides. This condition is that the electronic functions of the defect ion do not overlap the nearest lattice ions.

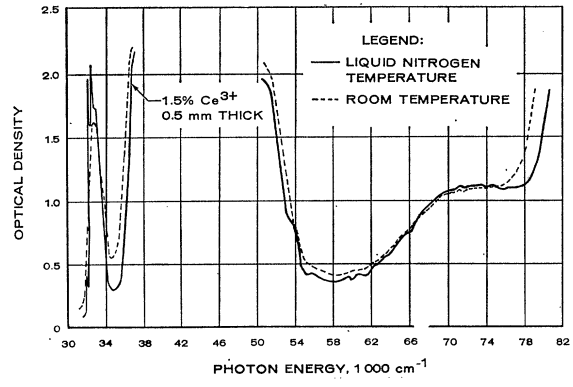
III. CONCENTRATION DEPENDENCE OF $4f \rightarrow 5d$ ABSORPTION OF Ce^{3+} IN CaF_2 —THE EFFECT OF CRYSTALLINE ENVIRONMENT ON Ce^{3+} ABSORPTION IN ALKALINE-EARTH FLUORIDES

The ultraviolet absorption spectrum of Ce^{3+} in CaF₂ changes as the concentration of Ce^{3+} varies. This change is most striking in the spectral region of $4f \rightarrow 5d$. Figure 3 shows this concentration effect in a series of ultraviolet absorption spectra of Ce^{3+} in CaF₂ at varying concentrations from 0.005% to 5%. With increase in Ce^{3+} concentration the $4f \rightarrow 5d$ bands corresponding to previously assigned single-ion absorption of Ce^{3+} decrease in intensity while the bands in the intermediate energy region *C* and *D* grow steadily. We suggest that these high-concentration bands in *C* and *D*, with peaks between 40 000 cm^{-1} and 42 000 cm^{-1} in region *C* and peaks between 46 000 cm^{-1} to 47 000 cm^{-1} for region *D*, are the $4f \rightarrow 5d$ absorption bands of clustered Ce^{3+} ions in CaF₂. We call the Ce^{3+} ion in cluster the "cluster ion" and its absorption "cluster-ion absorption." As the concentration of Ce^{3+} increases, we assume that many Ce^{3+} ions with their charge compensator, the nearest interstitial F^- , tend to cluster with other pairs instead of dispersing randomly in the crystal. The dominance⁹ of the cluster-ion absorption over that of the single ion at even moderate Ce^{3+} concentration, e.g., 0.15% Ce^{3+} in Fig. 3, favors this assumption of cluster formation. In the cluster, Ce^{3+} ions occupy all the Ca^{2+} sites and are surrounded by two types of F^- ions, the first type at corners of the cube (substitutional F^-) the second type at the body centers of neighboring cells (interstitial F^-). With this model of cluster-ion Ce^{3+} in heavily doped CaF₂ ($\geq 0.1\%$), we expect that the energy of the t_{2g} orbital of cluster-ion Ce^{3+} would remain higher than that of e_g , but the energy difference between them should be reduced because of the presence of the interstitial F^- in the e_g direction. We therefore assign the single band with peak between 46 000 to 47 000 cm^{-1} as the t_{2g} band and the composite band between 38 000 and 44 000 cm^{-1} as the e_g band. The crystal field strength, $10 Dq$, based on this assignment is about 5000 cm^{-1} , about one-half that of single-ion Ce^{3+} in CaF₂. The centroid of the $5d$ levels of the cluster ion is at about 45 000 cm^{-1} . This is about 3000 cm^{-1} lower than that of single-ion Ce^{3+} (see Table I) in CaF₂ and is presumably due to slightly larger dielectric screening around the cluster ion. The complicated

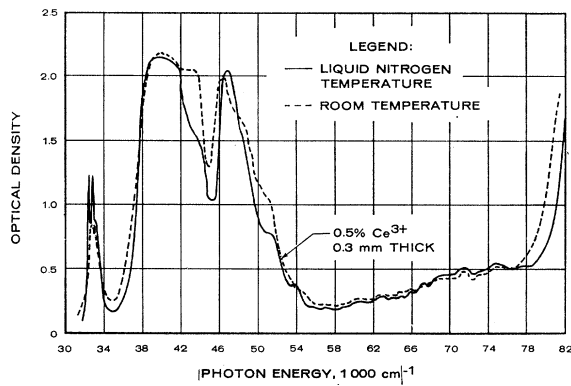
⁹ The spectra of 0.15% Ce^{3+} and 0.05% Ce^{3+} in Fig. 3 provide obvious comparison between the cluster-ion and single-ion absorption of Ce^{3+} . The product of (Ce^{3+} concentration) (sample thickness) for these two spectra is only 10% off, (0.05%) (0.78 mm) and (0.15) (0.29 mm), respectively.



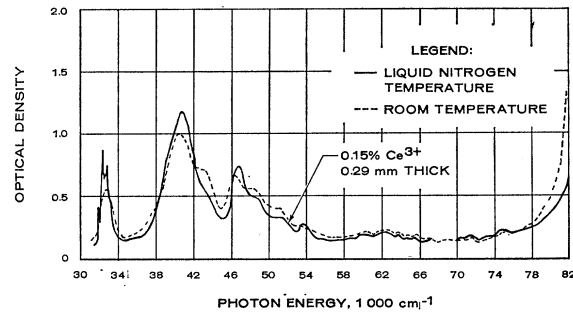
(a)



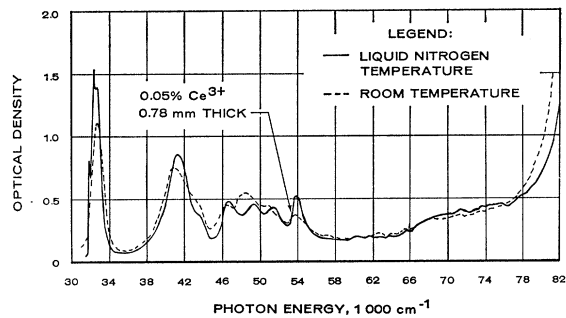
(b)



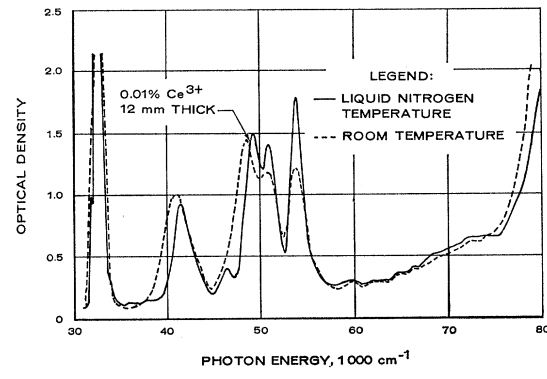
(c)



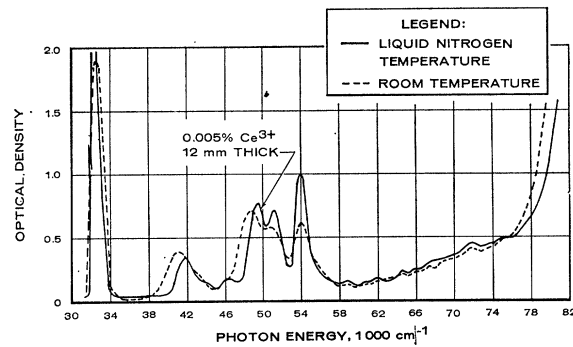
(d)



(e)



(f)



(g)

FIG. 3. Ultraviolet absorption spectra of Ce^{3+} in CaF_2 crystal at concentrations from 0.005% to 5% at room and liquid-nitrogen temperature.

nature of the e_g band in region C may be tentatively interpreted as follows. In the e_g direction there are neighboring cluster ions of Ce^{3+} sitting on the opposite side of the interstitial F^- ions. Two cluster ions 180° apart may be coupled together by superexchange via an interstitial F^- ion. The interaction between superexchange-coupled cluster ions in the e_g direction may split their e_g level. Transitions to these split e_g levels form the complicated e_g band in region C . The coupled ions presumably have far less splitting in the shielded $4f$ ground level. The thermal population on these moderately split $4f$ ground levels may be responsible for the temperature dependence of two main portions of the e_g band, e.g. the $41\,000\text{ cm}^{-1}$ and $44\,000\text{ cm}^{-1}$ peaks of 0.15% Ce^{3+} in Fig. 3.

Strong cluster-ion absorption of Ce^{3+} in SrF_2 is also anticipated when Ce^{3+} reaches comparable concentrations as in CaF_2 . This is indicated by the presence of similar absorption bands in the uv-absorption spectrum of 0.005% Ce^{3+} in SrF_2 as shown previously in Fig. 1. In BaF_2 there is, however, no appreciable cluster-ion absorption of Ce^{3+} even at 0.1% concentration in a 4-mm-thick sample. This lack of strong cluster-ion absorption in $BaF_2:Ce^{3+}$ may be attributed to the large interstitial dimensions of the BaF_2 lattice. A charge compensator F^- with ionic radius 1.33 \AA can easily fit into an interstice in the BaF_2 lattice where the ionic radius of Ba^{2+} is 1.43 \AA . This will result in small overlapping of the wave function of the interstitial F^- with those of the neighboring Ce^{3+} ions. The superexchange interaction, Ce^{3+} -interstitial F^- - Ce^{3+} , may therefore be weak in the BaF_2 crystal. On the other hand, the wave function of the interstitial F^- presumably will spill over the undersized interstices of the CaF_2 and SrF_2 lattice, with ionic radius of Ca^{2+} and Sr^{2+} being 1.06 \AA and 1.27 \AA , respectively, and overlap easily with neighboring Ce^{3+} ions. This may result in strong cluster-ion absorption via superexchange at sufficient Ce^{3+} concentration.

The interionic-distance dependence¹⁰ of superexchange interaction, which is inversely proportional to the tenth power of interionic distance, may also partially explain the weakness of cluster-ion absorption in $BaF_2:Ce^{3+}$. If this inverse tenth-power law¹⁰ is applicable to our model of the Ce^{3+} -interstitial F^- - Ce^{3+} , then the superexchange interaction will be in the ratio of $(2.35\text{ \AA})^{-10}$: $(2.49\text{ \AA})^{-10}$: $(2.71\text{ \AA})^{-10} = 1:0.5:0.25$ in CaF_2 , SrF_2 and BaF_2 lattice, respectively.

The effect of Ce^{3+} concentration on the low-temperature structure in the $|x^2-y^2\rangle$ band of single-ion Ce^{3+} in CaF_2 is shown in Fig. 4, which reproduces the lowest bands of Fig. 3 on the expanded photon energy scale. The concentration range, 0.005% to 5% , covered by our measurement may be divided into three regions according to their distinctive features in the low-temperature structure of $|x^2-y^2\rangle$ band. *First* is the low-concentration region as characterized by curves with Ce^{3+}

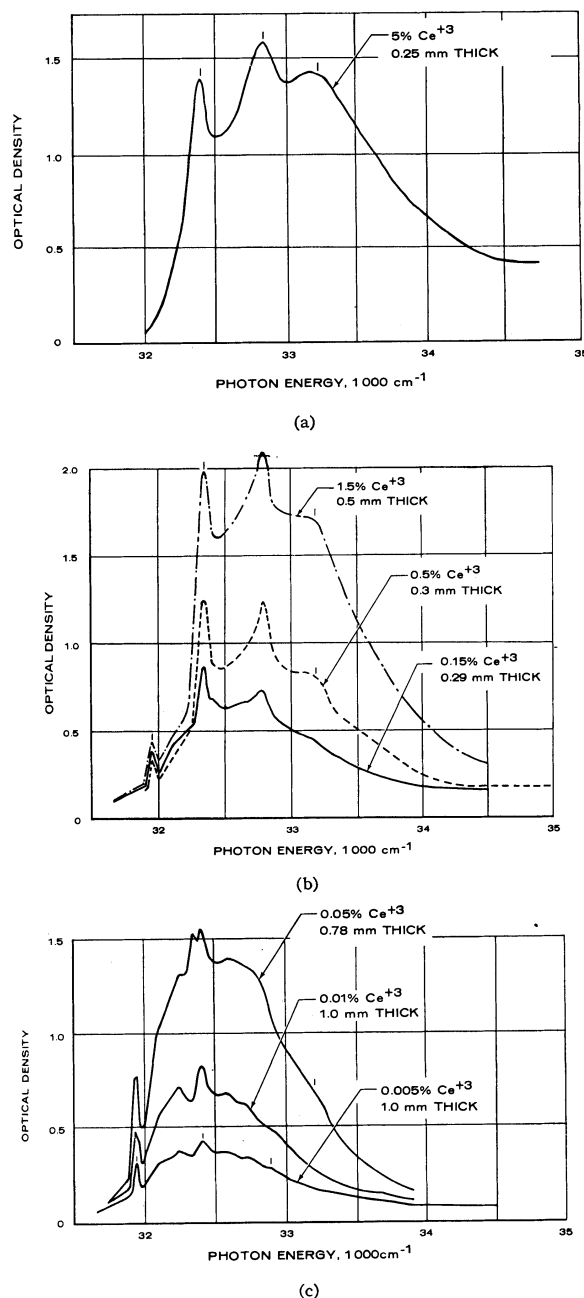


FIG. 4. The lowest $4f \rightarrow 5d$ absorption band of Ce^{3+} in CaF_2 crystal at concentrations from 0.005% to 5% at liquid-nitrogen temperature.

concentration up to $\sim 0.01\%$. As previously discussed, the structure in this low-concentration region is characterized by a zero-phonon peak at $\sim 31\,940\text{ cm}^{-1}$ followed by vibronic peaks separated with two frequency intervals, a large $\omega_1 = 460\text{ cm}^{-1}$ and a smaller $\omega_2 = 160\text{ cm}^{-1}$ within ω_1 (ω_1 and ω_2 are the resonance frequencies of the pseudolocalized vibration at the Ce^{3+} defect). The *second* is the region of intermediate concentration, between $\sim 0.5\%$ and $\sim 1.5\%$ as represented by

¹⁰ D. Bloch, J. Phys. Chem. Solids **27**, 881 (1966).

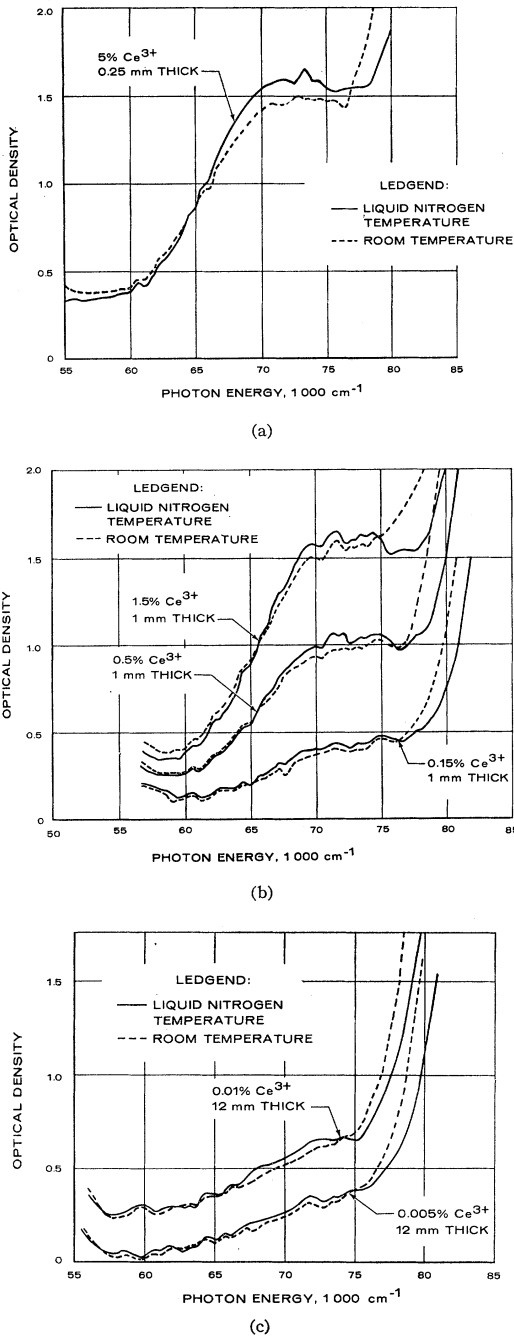


FIG. 5. Ultraviolet absorption spectra, between $60\,000\text{ cm}^{-1}$ and $80\,000\text{ cm}^{-1}$, of Ce^{3+} in CaF_2 crystal at concentrations from 0.005% to 5% at room and liquid-nitrogen temperature.

corresponding curves in Fig. 4. The zero-phonon peak in this intermediate-concentration region remains at $\sim 31\,940\text{ cm}^{-1}$ within the accuracy of our measurement. Three "major" peaks at $32\,340$, $32\,800$, and $33\,200\text{ cm}^{-1}$ in the structure seem to shift toward the zero-phonon peak. The corresponding ω_1 's are 400 cm^{-1} , 460 cm^{-1} and 400 cm^{-1} , respectively. The "minor" peaks are not

noticeable at liquid-nitrogen temperature, except possibly the first peak which is 160 cm^{-1} from the zero-phonon peak. The *third* region is for high Ce^{3+} concentration as shown by the absorption curve of 5% Ce^{3+} . Here neither the zero-phonon peak nor "minor" peaks are noticeable at liquid-nitrogen temperature. Three "major" peaks appear to shift back toward high energy as in the region of low concentration. They are at $\sim 32\,400\text{ cm}^{-1}$, $\sim 32\,850\text{ cm}^{-1}$ and $\sim 33\,230\text{ cm}^{-1}$. No attempts have been made to interpret the structure in the last two concentration regions.

IV. $4f \rightarrow 6s$ ABSORPTION OF Ce^{3+} IN CaF_2

We now discuss the uv absorption of Ce^{3+} in CaF_2 at energies higher than that of $4f \rightarrow 5d$. For this purpose Fig. 5 summarizes the spectra of Ce^{3+} in CaF_2 between $60\,000\text{ cm}^{-1}$ and $80\,000\text{ cm}^{-1}$ at concentrations from 0.005% to 5%. As Ce^{3+} concentration increases two types of absorption become increasingly obvious. First, above the background absorption near the cutoff of the host CaF_2 , there is a broad-band absorption between $\sim 60\,000\text{ cm}^{-1}$ and $77\,000\text{ cm}^{-1}$ with maximum at $\sim 70\,000\text{ cm}^{-1}$. This broad-band absorption is not observed in CaF_2 doped with other trivalent rare-earth ions such as Pr^{3+} and is therefore due to Ce^{3+} absorption. It is roughly proportional to the concentration of Ce^{3+} and the thickness of the sample. The band increases in absorption and sharpens at low temperature as shown by solid curves in Fig. 5. We estimate the oscillator strength of this broad-band absorption to be about two orders of magnitude smaller than that of combined $4f \rightarrow 5d$ bands in the region $31\,000\text{ cm}^{-1}$ to $56\,000\text{ cm}^{-1}$. This estimation is made by comparing the area of the corresponding absorption bands shown in Fig. 3. The weakness of this broad-band absorption suggests that it should be assigned as the $4f \rightarrow 6s$ absorption band with change of orbital number $f-s=3-0=3$ instead of $4f \rightarrow 5g$ with $g-f=4-3=1$ for strong absorption.

Table III compares the interconfigurational transition energies, $4f \rightarrow 5d$ and $4f \rightarrow 6s$, of free ion¹¹ Ce^{3+} with that of single-ion Ce^{3+} in CaF_2 . The last column in the table shows the ratio of the transition energy of the free ion to that of single-ion Ce^{3+} in CaF_2 . It shows the free ion-to-crystal ion ratio for $4f \rightarrow 6s$ transition is larger than that for $4f \rightarrow 5d$. This is presumably due to increasing dielectric screening of the extended $6s$ orbital of Ce^{3+} in CaF_2 .

TABLE III. Energy of centroid of $4f \rightarrow 5d$ and $4f \rightarrow 6s$ of free-ion Ce^{3+} and single-ion Ce^{3+} in CaF_2 .

Transition	Free-ion Ce^{3+}	Single-ion Ce^{3+} in CaF_2	(Free-ion Ce^{3+}) / (Single-ion Ce^{3+} in CaF_2)
$4f \rightarrow 5d$	$51\,000\text{ cm}^{-1}$	$48\,000\text{ cm}^{-1}$	1.06
$4f \rightarrow 6s$	$86\,600\text{ cm}^{-1}$	$70\,000\text{ cm}^{-1}$	1.24

¹¹ R. L. Lang, Can. J. Res. 14A, 127 (1936).

The possibility that either the observed $4f \rightarrow 6s$ broad band or the previously discussed $4f \rightarrow 5d$ cluster-ion absorption may be attributed to charge transfer of $F^-(2p^6) \rightarrow Ce^{3+}(4f)$ is ruled out. The energy of the $F^-(2p^6) \rightarrow RE^{3+}(4f)$ should successively decrease¹² as we progress through RE^{3+} ions varying from Ce^{3+} to Pr^{3+} , Nd^{3+} , ... to Eu^{3+} . We failed to notice corresponding low-energy absorptions in, for example, Pr^{3+} -doped alkaline-earth fluorides over a wide doping range.

V. RED SHIFT OF ABSORPTION EDGE OF $CaF_2:Ce^{3+}$

The second type of high-energy uv absorption in $CaF_2:Ce^{3+}$ occurs at the absorption edge of the host CaF_2 . Figure 5 shows that the absorption edge of CaF_2 , near $80\,000\text{ cm}^{-1}$, shifts toward low photon energy steadily as Ce^{3+} concentration increases.¹³ Since the absorption edge of strongly ionic crystal CaF_2 is usually interpreted¹⁴ as charge transfer from $F^-(2p^6)$ to $Ca^{2+}(4s)$, we interpret¹³ this apparent red shift of absorption edge of $CaF_2:Ce^{3+}$ with respect to the undoped CaF_2 as charge transfer from $F^-(2p^6)$ to $Ce^{3+}(6s)$.

The temperature effect on the absorption edge of $CaF_2:Ce^{3+}$ is similar to that of undoped CaF_2 . The absorption edge shifts toward higher energy at low

temperature as shown by solid curves in Fig. 5, presumably because of the contacting host lattice.

VI. CONCLUSION

The ultraviolet absorption spectra of Ce^{3+} in alkaline-earth fluorides may be divided into regions of three types of transitions: (1) $4f \rightarrow 5d$, about 2000 cm^{-1} wide at $10^{-2}\%$ Ce^{3+} , strong bands between $31\,000\text{ cm}^{-1}$ and $56\,000\text{ cm}^{-1}$; (2) a weak, broad $4f \rightarrow 6s$ band between $60\,000\text{ cm}^{-1}$ and $77\,000\text{ cm}^{-1}$; and (3) the onset of charge transfer $F^-(2p^6) \rightarrow Ce^{3+}(6s)$ which is noted as an apparent red shift of the band edge of the host crystal, for example, in CaF_2 near $80\,000\text{ cm}^{-1}$.

The vibronic structure in the lowest $4f \rightarrow 5d$ transition may be speculated in terms of pseudolocalized vibrations at the Ce^{3+} defect as in the case of RE^{2+} ions in alkali halides. The concentration effect on the spectra is interpreted as cluster-ion absorption at Ce^{3+} concentrations $\geq 0.1\%$.

The present interpretation of the ultraviolet absorption spectra of Ce^{3+} in alkaline-earth fluorides may be strengthened by other related measurements. These are, for example, electron spin resonance on the local symmetry of Ce^{3+} ions in our samples, similar absorption measurements on similar systems such as RE^{2+} ions in alkali halides, and/or on slightly dissimilar host such as good quality $LaF_3:Ce^{3+}$ crystals, where the charge compensation and therefore cluster formation may be absent.

ACKNOWLEDGMENTS

The author is grateful to Hughes Research Laboratories, where the measurements were performed. He is indebted to the late beloved G. Dorosheski for the tireless computation and construction of numerous graphs. Crystals were supplied by Optovac, Inc. J. R. Henderson has kindly read the manuscript. This work was partly supported by the Douglas Independent Research and Development Program.

¹² C. K. Jørgensen, *Mol. Phys.* **5**, 271 (1962); in Proceedings of the 5th Rare Earth Research Conference, Ames, Iowa, 1965 (unpublished).

¹³ The broad $4f \rightarrow 6s$ absorption band around $70\,000\text{ cm}^{-1}$ may contribute to the red shift of the absorption edge in Fig. 5. However, we have observed that this red shift is quite general in samples doped with other RE^{3+} ions such as Pr^{3+} and Nd^{3+} , where there is no absorption band such as $4f^n \rightarrow 6s4f^{n-1}$ in the neighborhood of the absorption edge. This general nature of the apparent red shift of the absorption edge of RE^{3+} doped CaF_2 crystals leads us to rule out the possible interpretation of $F^-(2p^6) \rightarrow RE^{3+}(4f^n)$ or $F(2p^6) \rightarrow RE^{3+}(5d)$. This is because, for example, the energy of $F^-(2p^6) \rightarrow RE^{3+}(4f^n)$ is RE^{3+} -dependent. (See Ref. 12.) The transition of $F^-(2p^6) \rightarrow RE^{3+}(5d)$ presumably will also depend on RE^{3+} ions.

¹⁴ See, for example, R. S. Knox, *Solid State Phys. Suppl.* **5**, 61 (1963).